DALTON
FULL PAPER

Supramolecular assembly of metalloporphyrins in crystals by axial coordination through amine ligands

Yael Diskin-Posner, Goutam Kumar Patra and Israel Goldberg *

School of Chemistry, Sackler Faculty of Exact Sciences, Tel Aviv University, 69978 Ramat Aviv, Tel Aviv, Israel. E-mail: goldberg@post.tau.ac.il

Received 5th June 2001, Accepted 1st August 2001
First published as an Advance Article on the web 12th September 2001

Axial coordination to metalloporphyrins is an important tool in the supramolecular chemistry of these entities. Metalated 5,10,15,20-tetraphenylporphyrins can be axially linked to each other with the aid of amine and diamine ligands. Seven new crystalline materials consisting of such heterogeneous coordination oligomers and polymers of Zn(II)– or Mn(III)–tetraphenylporphyrins have been prepared and characterized by X-ray crystallography. Ligands of varying length have been used as bridging auxiliaries between the metal centers of the porphyrin species, effecting heterogeneous porphyrin-ligand oligomeric as well as polymeric assemblies. These correspond, respectively, to "wheel-and-axle" and "shish-kebab" type shapes of the supramolecular scaffolds. In addition, a uniquely structured homogeneous coordination polymer of a Zn(II)–tetrapyridylporphyrin derivative, is also reported.

1 Introduction

The important role played by metalloporphyrins in mediating electron and energy transfer, their utility as redox catalysts, and their dynamic photophysical properties,[1] have stimulated extensive interest in the supramolecular chemistry of these systems and the design of diverse multiporphyrin architectures. Directed metal–ligand coordination is one of the most effective means of formulating stable organometallic nanostructures in solution and thin layers, as well as of polymeric assemblies in the solid state.[2] Such materials were shown to be relevant for a variety of potential applications, *e.g.* as photophysical sensors,[3] nanoscopic devices,[4] organic magnets[5] or even as structural and functional analogs of inorganic zeolites.[6] Among several other possible auxiliaries that can bind two or more metalloporphyrin units into a supramolecular aggregate, aliphatic and aromatic amines proved particularly useful linkers due to their high affinity for transition metals. Linear multiporphyrin assemblies can be readily achieved by the axial coordination of diamines, such as the 4,4′-pyridines, to the metal centers of adjacent metalloporphyrins. The nature of the metal and the length and shape of the ligand spacer provide additional variants of the supramolecular structure. In this work we expand on earlier observations by us as well as by others on this subject,[7,8] and report eight new solid structures of oligomeric and polymeric metalloporphyrin entities. These are based on zinc tetraphenylporphyrin (Zn^{II}TPP, **1a**), and manganese tetraphenylporphyrin ($Mn^{III}TPP^{+}$, **1b**) building blocks that are joined together by diverse amine and diamine ligands (**2**–**7**) not used before to this end (Scheme 1). The ability of the zinc–porphyrins to form continuous single-component coordination polymers by axial coordination, rarely observed in earlier studies, is of particular interest. The present investigation reveals a new self-assembled coordination polymer of the zinc tetrapyridylporphyrin (Zn^{II}TPyP, **1c**) type.

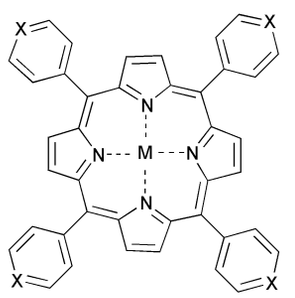

(1a) M = Zn; X = C–H
(1b) M = Mn; X = C–H
(1c) M = Zn; X = N:

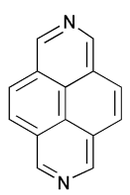

(2)

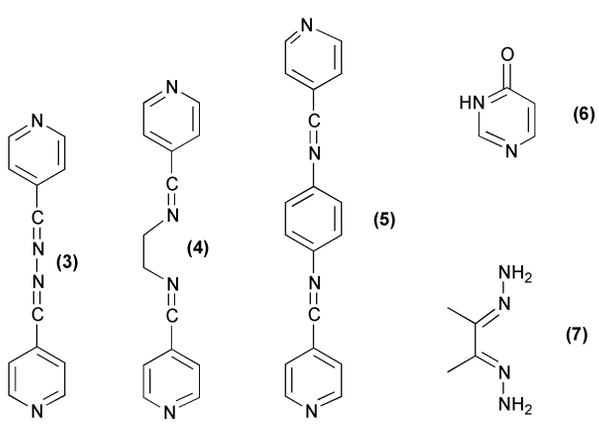

Scheme 1

2 Results and discussion

The following porphyrin-based coordination oligomers and polymers in the solid state were prepared and structurally analyzed in this study; due to the non-self-complementary shapes of these compounds,[9] they all crystallized as either nitrobenzene or chloroform solvates: **8** [2(**1a**)·(**2**)·4($PhNO_2$)], **9** [2(**1a**)·(**3**)·7($PhNO_2$)], **10** [2(**1a**)·(**4**)·4($PhNO_2$)], **11** [2(**1a**)·(**5**)·2($CHCl_3$)], **12** [2(**1a**)·2(**6**)·5($PhNO_2$)], **13** [(**1b**·ClO_4)·(**3**)·3($PhNO_2$)], **14** [(**1a**)·(**7**)·2($PhNO_2$)], **15** [2(**1c**)·5($PhNO_2$)]. Geometric details of the coordination interactions in all the compounds are listed in Table 1.

2.1 Coordination oligomers

From among the known metalloporphyrins, ZnTPP was found particularly suitable for the formation of ordered

DOI: 10.1039/b104961p

Table 1 Selected bonding and coordination distances in structures **8**–**15**

Compound	Interporphyrin spacing[a]/Å	M[b]–N(porphyrin) bond length range/Å	M[b]–N(ligand) distance/Å	M[b] deviation from porphyrin plane[a]/Å
8	11.5	2.054–2.078(2)	2.196(2)	0.26
9	15.85[c]	2.066–2.074(2)	2.147(2)	0.28[c]
		2.065–2.076(2)	2.164(2)	
10	14.3	2.055–2.078(2)	2.198(2)	0.28
11	20.5	2.062–2.087(3)	2.167(4)	0.33
12	10.7	2.053–2.074(2)	2.237(2)	0.26
13	15.7	1.998–2.024(4)	2.338(4)	0.01[d]
			2.339(4)	
14	7.7	2.026–2.120(4)	2.272(5)	0.28
15	19.9	2.061–2.095(7)	2.336(6)	0.02[d]
			2.378(6)	
		2.052–2.076(7)	2.121(8)	0.29

[a] Reference was made to distances from the mean plane(s) defined by the four pyrrole nitrogen atoms in each porphyrin entity. [b] M refers to Zn(II), except for **13** where it is Mn(III). [c] A mean value is shown for the two crystallographically independent distances. [d] Six-coordinate metal ions. In all other cases shown the Zn(II) ions are five-coordinate.

supramolecular nanostructures by axial intercoordination.[8,10] A literature survey revealed that the zinc ion in the porphyrin center has a marked preference for either four-coordinate square-planar, or five-coordinate square-pyramidal environments. It binds to the four inner pyrrole nitrogens of the porphyrin macrocycle and quite often also to another ligand in the axial direction, revealing a particularly high affinity for nitrogen Lewis bases. Suitably shaped bidentate diamine ligands can, therefore, be used effectively for the realization of rigid ligand-bridged porphyrin dimers, in which the ligand auxiliary is sandwiched between two porphyrin macrocycles. We have demonstrated in an earlier publication several formulations of such ZnTPP-based oligomeric crystalline structures, applying a series of diaminoalkane and bipyridyl-type functional ligands.[8] The ligands varied from one another mainly by the length of the ligand spacer, with the distance between the two porphyrin components in the assembly spanning from 9.4 to 14.0 Å. Similar oligomers based on TPP frameworks with other metal ions and alternative ligands have also been reported.[8,10] In view of the as yet limited structural database of such systems, and the vast importance of axial coordination in the self-assembly processes of metalloporphyrins, we describe in this section the detailed structure of several additional systems of this type and describe their specific features. This includes reactions of ZnTPP (**1a**) with 2,7-diazapyrene (**2**), *N*,*N*′-bis(4-pyridylmethylidyne)hydrazine (**3**), *N*,*N*′-bis(4-pyridylmethylidyne) ethylene-1,2-diamine (**4**) and *N*,*N*′-bis(4-pyridylmethylidyne) phenylene-1,4-diamine (**5**), which yield the corresponding 2 : 1 oligomeric structures **8**, **9**, **10**, and **11**, respectively. The ligands are of increasing length, allowing the two porphyrin macrocycles to be placed at an unprecedented distance of more than 20 Å from each other (with the longest ligand) and still maintain a rigid "wheel-and-axle"-type geometry.

Fig. 1 illustrates the structure of **8**. The 2,7-diazapyrene is a bulkier and more rigid ligand than 4,4′-bipyridyl, which leads to the formation of a stable and well resolved structure. The oligomeric units interlock with one another, the porphyrin components forming a characteristic corrugated stacked arrangement throughout the crystal lattice. Molecules of nitrobenzene solvent are incorporated into the crystal between the interlocked units, being sandwiched between the concave surfaces of the porphyrin "wheels" as well as between neighboring diazapyrene frameworks. The zinc ion deviates by 0.26 Å from the plane of the four pyrrole nitrogens towards the axial ligand, and the interporphyrin distance within each aggregate is 11.5 Å (Table 1). The distance between the porphyrin cores of adjacent oligomers, which define the solvent enclosure (pairs of antiparallel nitrobenzene molecules, Fig. 1), are distant at about 7.5 Å from each other.

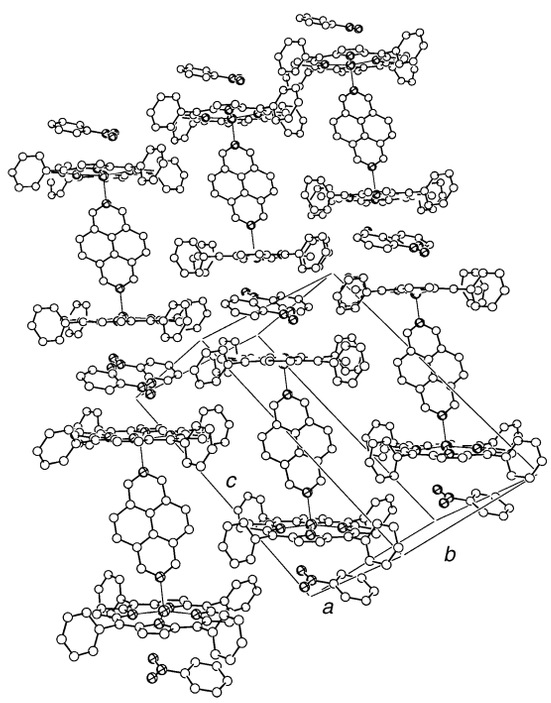

Fig. 1 Perspective view of the crystal structure of **8**, showing the organization of the ligand-bridged porphyrin dimers. It illustrates also the corrugated chain arrangement of the porphyrin components, as well as the occlusion of the nitrobenzene solvent between these chains. The nitrobenzenes located between the diazapyrene frameworks, and the hydrogen atoms are omitted for clarity. In this and in the following figures the metal–ligand coordinations and the frame of the unit-cell are indicated by thin lines, and all the non-carbon atoms (Zn, N, O, Cl) are marked by darkened circles.

Ligand **3** is aromatic and maintains a rigid planar geometry. Its rigidity facilitates the formation of a stable ligand-bridged porphyrin dimer **9** with ZnTPP (Fig. 2). The crystal structure of this material reveals similar features to those described in the previous example (interlocking of the trimeric assemblies into one another, corrugated-chain organization of the offset-stacked porphyrin components, and entrapment of nitrobenzene solvent in the intermolecular voids between the trimeric units). The two crystallographically independent entities in the asymmetric unit of this structure reveal that the interporphyrin distances within the oligomers are 15.8 and 15.9 Å (the zinc ions deviate 0.28–0.29 Å from the porphyrin plane towards the ligand), considerably longer than has been characterized before. The oligomeric moieties still maintain a perfect

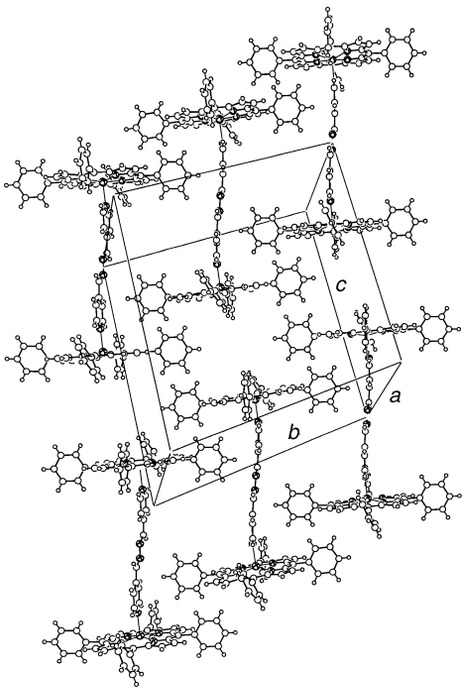

Fig. 2 Crystal structure of **9**, illustrating the geometry of the coordination oligomers as well as the spaces between them at the interfaces of the corrugated porphyrin chains and along the "thin" bridging ligands. The partly disordered molecules of nitrobenzene, that fill these voids in the crystal, were omitted for illustrative purposes.

"wheel-and-axle" shape, the bridging bidentate ligand being aligned perpendicularly to the planes of the porphyrin units. The long linear ligand of each unit is surrounded by the phenyl groups of adjacent oligomers, as well as by molecules of the nitrobenzene solvent. The latter are also incorporated between the concave surfaces of adjacent oligomers displaced along the [101] axis of the crystal. Correspondingly the solvent content here is higher than in the previous example, with seven equivalents of nitrobenzene per ligand-bridged dimer in this structure, as opposed to four equivalents of nitrobenzene in the former example.

Elongation of **3** by placing an aliphatic $(CH_2)_2$ group between the two nitrogens yields a somewhat longer but more flexible ligand **4**, that also readily connects to two ZnTPP entities. The ligand flexibility allows adjustment of the oligomeric structure to surround most effectively the nitrobenzene molecules confined in the lattice (in a perfectly ordered manner, one pair between the concave surfaces of adjacent porphyrin wheels and a second pair between the bridging ligands of neighboring oligomers). The resulting crystal structure of this trimeric compound (**10**) is illustrated in Fig. 3. It shows the bent conformation of the ligand that effects a considerable parallel offset of the two porphyrin moieties within the oligomeric units. The distance between the two porphyrin planes within each such unit is in this case only 14.3 Å (Table 1).

It is still possible to obtain a similarly structured oligomeric entity even with a longer ligand spacer such as **5**. This ligand has an extended conformation, and in its complex with ZnTPP, **11**, it holds the two porphyrin frameworks at a distance of 20.5 Å from each other without any marked distortion of the "wheel-and-axle" geometry (Fig. 4). Such spacing is already wider than the size of the porphyrin "wheel", which results in an interesting modification of the intermolecular organization. Instead of the most dominant pattern observed before, in which all the porphyrin units are aligned parallel to each other (whether in triclinic or even in some monoclinic structures) in order to maintain the offset-stacked overlap,[11] in this structure neighboring oligomeric units are arranged in a perpendicular

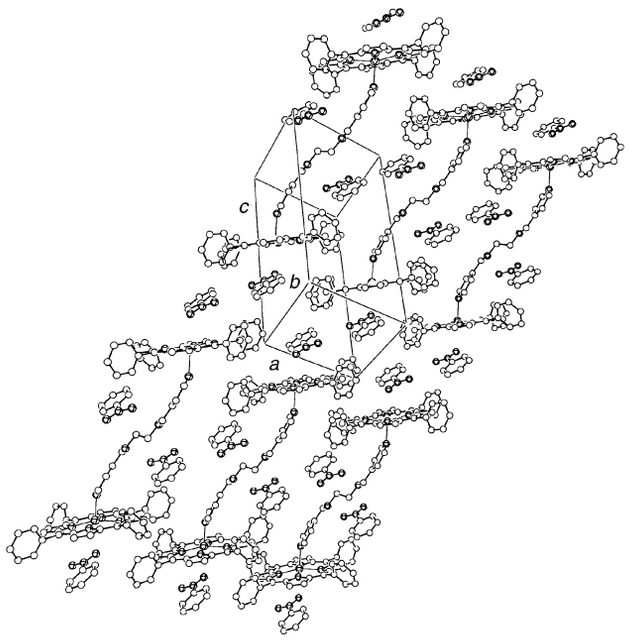

Fig. 3 Perspective view of the intermolecular organization in **10**. The solvent occluded between the oligomeric units is ordered and well characterized in this case, due to the flexibility of the bridging ligands. The H-atoms are omitted for clarity.

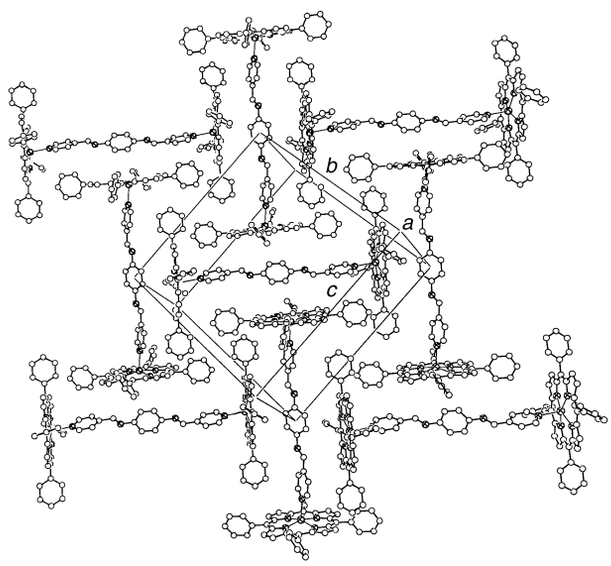

Fig. 4 Layered arrangement of the coordination oligomers in **11**, in which the porphyrin "wheels" are separated by more than 20 Å (which is more than the van der Waals diameter of the TPP framework) from each other. In this structure the oligomeric units are aligned perpendicularly to each other in order to optimize intermolecular dispersive interactions and occupation of space (rather than in a parallel fashion as in the previous examples). Disordered chloroform solvent (not shown) is located in the interface between adjacent layers.

manner. This allows the fitting of the porphyrin framework of one trimer into the interporphyrin spacing of an adjacent trimer unit, and thus fill space more effectively. In the resulting structure one set of oligomers extending, and mutually displaced, along the [111] axis of the crystal is interspersed by similar units oriented along a perpendicular direction. The linear ligand of the latter is trapped between the concave surfaces of the former, thus yielding a relatively condensed intermolecular arrangement with a relatively low content of interstitial solvent.

Nanostructures of a similar type can also be assembled by the interaction of **1a** with the 4(3*H*)-pyrimidone ligand (**6**),

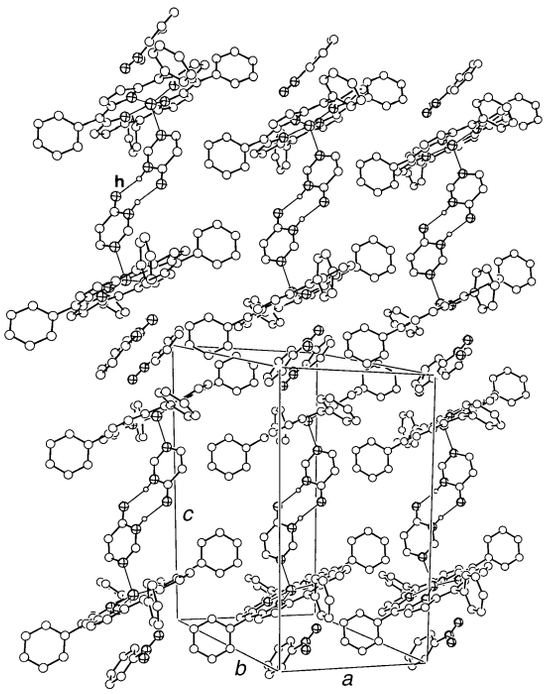

Fig. 5 Molecular structure and crystal packing of the ligand-bridged porphyrin dimers in **12**. Although the bridging moiety now consists of two H-bonded pyrimidone ligands (the H-bonds are marked by thin lines and at one site by "h"), the structural features characterizing the related oligomeric moieties in **8**–**10** are conserved in this structure as well. Disordered molecules of the solvent located between the H-bonding sites of adjacent species are omitted for clarity.

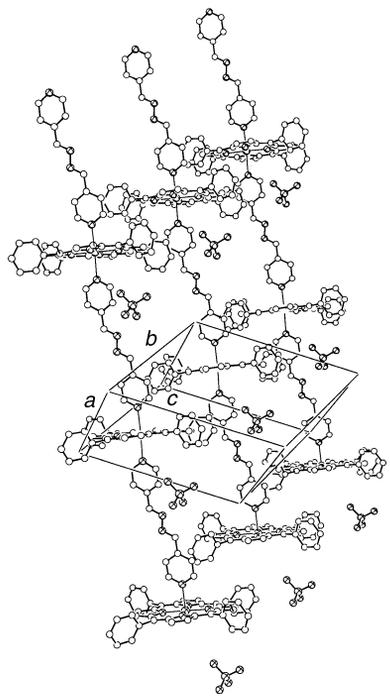

Fig. 6 MnTPP·ClO_4-based heterogeneous coordination polymers in **13**. Note the corrugated arrangement of the porphyrin fragments. The nitrobenzene solvent was omitted for clarity.

except that in this case the porphyrin : ligand stoichiometry of such clusters is 2 : 2, rather than 2 : 1. As in compounds **2**–**5**, the N(sp^2) site of **6** ligates readily to the porphyrin zinc ions. On the other hand, **6** tends also to dimerize by strong hydrogen bonding through the self-complementary NH–CO fragments.[11] The resulting crystal structure of the oligomers thus formed, **12**, is illustrated in Fig. 5. The oligomers consist of four different molecular species joined together by two Zn···N coordinations and two N–H···O hydrogen bonds. In order to accommodate simultaneously these two interaction types, the coordination to zinc as well as formation of the H-bonded pyrimidone dimers, the two porphyrin frameworks in the oligomeric cluster are shifted sideways parallel to each other. The axial distance between these frameworks is 10.7 Å, with the zinc ions of the two "wheels" being slightly displaced inward (Table 1).

2.2 Coordination polymers

Supramolecular coordination polymers of metalloporphyrins induced by axial coordination of bridging ligands to the core ions of the porphyrin species are much less abundant in the literature than their oligomeric counterparts. This can be attributed mainly to entropic effects: the relative instability of linear multiporphyrin arrays at ambient conditions (whether in solution or in the solid state), and the interference of competing ligands present in the reaction mixture (*e.g.*, solvents used to dissolve the interacting components such as water, methanol, *etc.*) which may block the axial ligation sites by associating with the metal ions. The construction of extended arrays with long range order is also hampered by the large size and limited flexibility of the porphyrin building blocks. Correspondingly, a relatively small number of ordered *polymeric* structures that involve metalloporphyrins has been reported thus far. Most of them incorporate derivatives of manganese porphyrin, as the Mn(III) ion exhibits a high propensity for a six-coordinate environment and affinity for binding either oxo-, cyano- or amine-ligands.[5] Some of the constructed manganese polymers have also revealed interesting magnetic properties.[5]

A typical example of a MnTPP-based linear coordination polymer is represented by compound **13**. This polymer is composed of porphyrin-**1b** perchlorate and the bipyridyl ligand **3**. The porphyrin core framework of **1b** is perfectly planar. The rigidity of the bridging ligand, and the effective side packing of adjacent polymeric chains yield a perfectly ordered structure (Fig. 6). Side packing of the linear polymers forms a corrugated arrangement of the porphyrin fragments, optimizing the porphyrin–porphyrin dispersive interactions. The voids between the thinner bridging ligand sections of adjacent polymers are filled by the perchlorate anions as well as by one mol of the nitrobenzene solvent. The distance between successive porphyrin planes along the polymeric chains is 15.7 Å, very close to the value observed in **9**. A similarly structured polymer of **1b** with a related 4,4′-bipyridyl ligand was reported by us earlier.[12]

It has been considerably more difficult to construct extended coordination polymers with the zinc tetraphenylporphyrin building blocks, due to the low affinity of the zinc ion for an octahedral ligation environment.[13] Only scattered examples of monomeric six-coordinate complexes of various zinc porphyrin derivatives with amine axial ligands have been characterized,[9,14] and even less so when it comes to their extended polymers.[15] This five- *vs.* six-coordination "dilemma" of the zinc ions is beautifully illustrated by compound **14** that was constructed by reacting **1a** with the 2,3-butanedione dihydrazone ligand **7**. The NH_2 ligating sites of the latter have to approach the porphyrin core in an inclined fashion in order to expose the lone-pair electrons of their terminal nitrogens to interactions with the zinc ions. Fig. 7a shows the polymeric arrangement that formed in this structure and the diagonal approach of **7** with respect to adjacent porphyrin frameworks. This relative inclination of the ligand places the adjacent porphyrin cores along the polymeric chain at 7.7 Å from each other. Careful inspection of the crystallographic results reveals, however, that the zinc ions do not reside in the center of the porphyrin planes. Rather, they are disordered about the center, being displaced either up or down

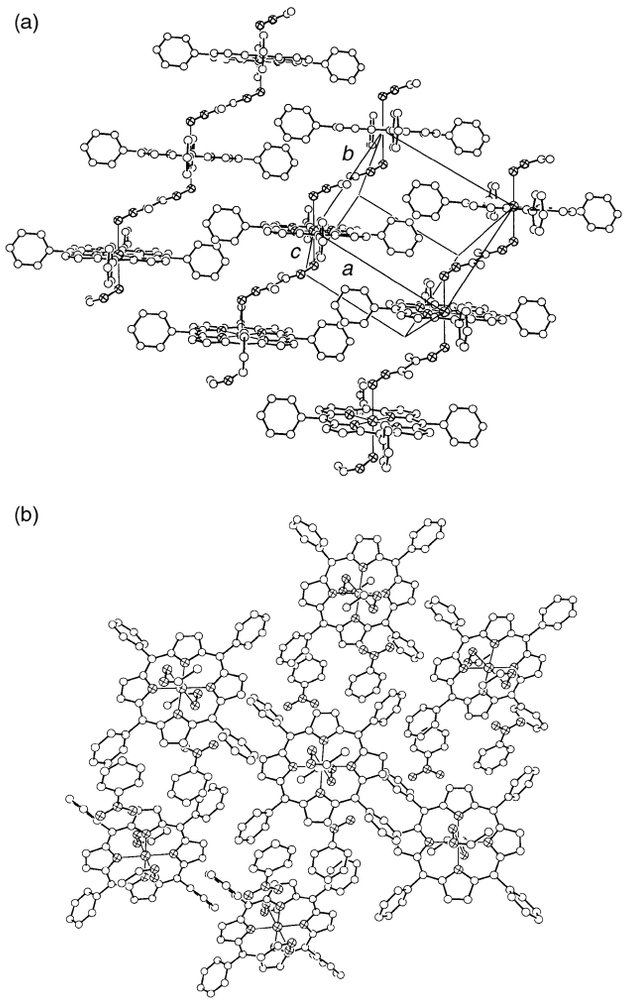

Fig. 7 ZnTPP-based heterogeneous extended coordination polymers in **14**. The zinc ion shown in the porphyrin center is essentially disordered about it, being located either above or below the porphyrin plane. (a) Side packing of the polymeric entities. (b) Projected view approximately down the polymer axes, showing the location of the nitrobenzene solvent within interstitial voids between the polymeric chains.

from it. In the refined structural model the porphyrin species are located on centers of inversion, but their zinc ions reveal a twofold disorder about them, deviating 0.28 Å from the porphyrin plane in either direction (see Experimental section).

Thus, compound **14** provides a unique manifestation of a linear polymeric assembly of the constituent species, while maintaining an essentially six-coordinate [5 + 1] environment of the central zinc ions at any given site. The zinc disorder can be either static or dynamic. In the former case, at every porphyrin site the zinc ion is surrounded by the pyrrole N-atoms at 2.026–2.120(4) Å, the coordinated amine at 2.272(5) Å, and the inversion-related amine approaching the "back" concave side of the porphyrin core at 2.812(6) Å (the distance of the porphyrin center to the two surrounding amines is 2.540 Å). In the latter case the $Zn \cdots NH_2$ distance varies between these two values. Fig. 7b depicts the relative displacement of adjacent polymeric chains in the crystal and the interstitial location of the nitrobenzene solvent.

The known examples of polymers constructed from zinc–porphyrins through axial coordination, in which the zinc ion shows a genuinely octahedral coordination, involve ZnTPyP (**1c**) and its tetracyanophenyl analog (ZnTCNPP) as building blocks.[15] ZnTPyP and ZnTCNPP already have N-ligation sites (pyridyl or cyano groups) incorporated into them, and construction of these polymers could, therefore, be achieved as homogeneous self-assembled arrays without resorting to external ligand auxiliaries. In the context of the present investigation we attempted the construction of ligand bridged crystalline oligomers or polymers with the tetrapyridyl **1c**, following the successful examples based on the **1a** and **1b** building blocks (see above). However, these efforts have failed thus far. Instead, crystals that emerged from one of the preparative experiments with **1c** and the diamine ligands yielded a new homogeneous coordination polymer of this porphyrin of previously unknown architecture, **15**. Our earlier studies have shown that when the zinc is five-coordinate, **1c** may form one-dimensional polymeric aggregates (where every porphyrin unit links to two other units, one bond is made through the zinc ion and the other bond is made through one of the peripheral pyridyl sites).[15] When it is six-coordinate, a three-dimensional coordination pattern forms in which every porphyrin framework is bound axially to two adjacent units through the zinc and equatorially to two additional porphyrins through two *trans*-related pyridyl substituents. In **15** an intermediate and unique situation occurs (Fig. 8). The polymeric arrays in this compound are composed of two crystallographically independent porphyrin units oriented perpendicularly to one another, one with a five-coordinate and the other with a six-coordinate zinc ion. They are arranged in an alternating manner along the polymer. Every building block has three connections to the neighboring molecules. The six-coordinate porphyrin links axially to two five-coordinate species located on opposite sides of its planar core ring, and laterally through one of its pyridyl rings to another five-coordinate moiety (Fig. 8). Simultaneously, every five-coordinate molecule associates with three six-coordinate porphyrins, through two of its *trans*-related pyridyl rings as well as by attracting the pyridyl group of another unit to its central zinc ion. The axial $Zn \cdots N(py)$ interactions are 2.336–2.378(6) Å and 2.121(8) Å for the six- and five-coordinate ions, respectively. This binding mode creates "ladder"-type polymeric assemblies of **1c** which are arranged in this structure parallel to each other along the *c* axis of the crystal. There are open interporphyrin voids within the ladders around $(x,½,0)$ and $(x,½,½)$, the spacing between the inner van der Waals surfaces across these voids being approximately 4 × 5 $Å^2$. Parallel stacking of the polymers along the *a* axis of the crystal creates continuous channels that propagate in this direction. The latter are accommodated by numerous molecules of disordered nitrobenzene solvent.

2.3 Additional evaluations and concluding remarks

This study (along with the earlier observations[2,5,7,8,15]) demonstrates effective assembly processes of heterogeneous oligomers, as well as heterogeneous and homogeneous polymers, by axial coordination of various amine ligands to metalloporphyrins, and provides a detailed structural characterization of these materials. In several respects the crystal packing of the assembled solids is similar to that observed in the large majority of common clathrates of monomeric ZnTPP's.[9] Thus, the dominant structural motif in the triclinic structures (**8**–**10**, **12**, **13**) is characterized by an interlocked arrangement of the porphyrin aggregates, showing a largely conserved corrugated pattern of offset-stacked porphyrin components at typical intervals of about 4.5–5.0 Å between neighboring species. The latter represents a fundamental property of the porphyrin–porphyrin interaction, and is little affected by the geometric constraints introduced by the bridging ligands.[8,9] The layered pattern of nearly parallel porphyrin species is also preserved in compound **14**, which is characterized by a monoclinic space symmetry (Fig. 7). It is possible to induce other modes of the intermolecular organization by using functional linkers equal to, or larger than, the porphyrin building block (*e.g.*, another porphyrin entity or a long diamine ligand). This is illustrated by compounds **11** and **15**. These structures consist of two groups

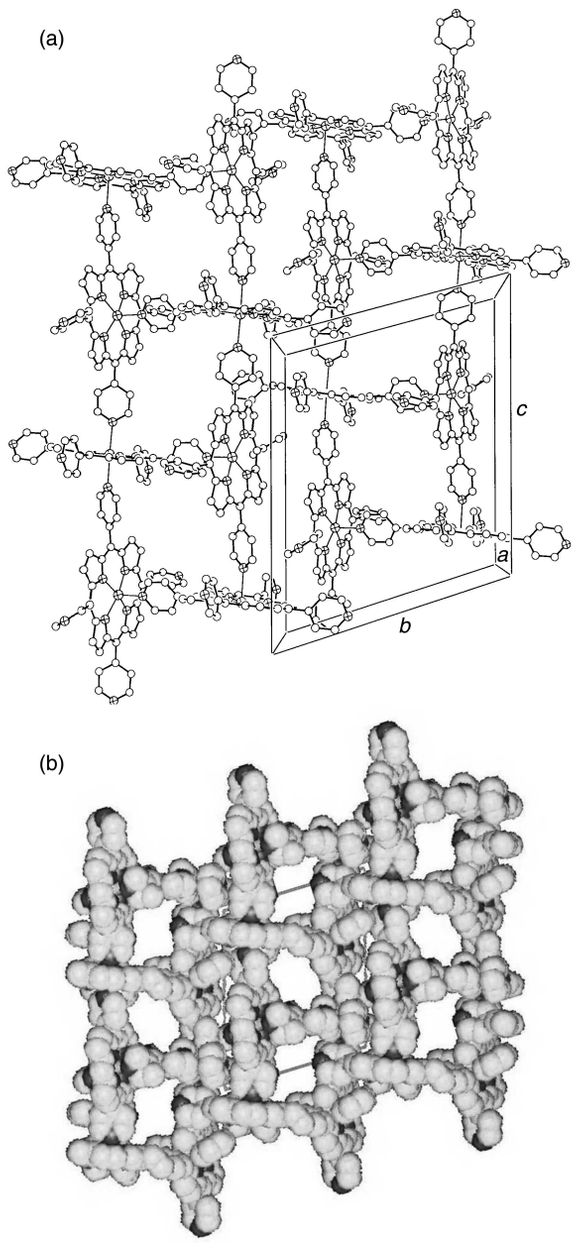

Fig. 8 (a) Homogeneous ladder-type coordination polymer composed of the ZnTPyP building blocks in **15**. It propagates along the *c* axis of the crystal. Two neighboring polymers displaced by *b* are shown to indicate their interlocked arrangement. (b) Space-filling model of the crystal structure projected down the *a* axis of the crystal, showing continuous interporphyrin channel voids in the lattice centered at (x,½,0) and (x,½,½). These channels are partly occupied by disordered molecules of the solvent (not shown).

of almost perpendicularly oriented porphyrin frameworks, one unit acting as spacer between two other units.

As the supramolecular porphyrin arrays are not self-complementary in three-dimensional space, successful formation of their ordered solids is influenced also by the nature of the crystallization environment. Noteworthy in this context are the following features. Nitrobenzene was found to be a very (if not the most) effective solvent in crystallizations of supramolecular multiporphyrin materials.[6,16] In the five-coordinate ZnTPP-based compounds it provides an excellent auxiliary to interact with the porphyrin framework, being located nearly parallel, and in close proximity, to the concave side of its central core. The rigidity and polarity of the aromatic nitrobenzene molecule also seem to play a significant role in stabilizing open multiporphyrin architectures in crystals by interacting with the molecular surface of the aromatic substituents on the porphyrin core and often efficiently filling the intermolecular voids. Another important observation relates to the induced growth of "porous" extended arrays which are difficult to form by standard crystallization techniques. For example, the construction of stable homogeneous multiporphyrin networks with very wide 1.5 nm channels could be realized (using the zinc–tetracarboxyphenylporphyrin building blocks and self-complementary H-bonding between them) when crystallization was attempted not directly from the nitrobenzene solvent, but in the presence of another inert component around which the open assembly may nucleate (the structure thus induced then grows without this component). This additional component also prevents excessive solvation of the porphyrin building blocks by the nitrobenzene molecules by diluting the solvent. A phenomenon of similar nature seems to have occurred in the formation of **15**. While stoichiometric amounts of **1c** and **3** were used in this experiment with the expectation of assembling a heterogeneous array as in the other examples (see above), a porphyrin-only coordination polymer with a "porous" architecture formed. Both the porphyrin as well as the ligand species have pyridyl sites available for axial coordination to the zinc, and entropy effects could favor the heterogeneous assembly. It appears nevertheless, that in this case the linear and thin bipyridyl ligand served as a nucleator (rather than as a bridging agent) for the assembly of the unusually shaped polymer of **1c**. The resulting crystal structure resembles a molecular sieve material with sizeable channels accessible to other species. The latter propagate through the crystal parallel to the porphyrin plane along the *a* axis of the unit-cell and are filled with numerous molecules of uncoordinated solvent.

The above findings provide characteristic examples of the supramolecular assembly of metalloporphyrins through axial coordination, and add useful information for further crystal engineering efforts of multiporphyrin nanostructures and extended arrays.

3 Experimental

Materials

Porphyrins **1a**, **1b** (as their perchlorate salts)[17] and **1c** were purchased from Porphyrin Systems GbR, and used as received. All starting materials for the ligand syntheses, common solvents, as well as compound **6** were purchased from Aldrich and used as received.

Preparative procedures

Compounds **2**, **3** and **7** are known, and were synthesized by following the literature documented procedures.[18–20] The same methodology was applied in the synthesis of **4** [anal. found (calc.): C, 70.43 (70.56%); H, 5.76 (5.92%); N, 23.62 (23.52%); yield 61%] and **5** [anal. found (calc.): C, 75.39 (75.50%); H, 4.94 (4.93%); N, 19.46 (19.57%); yield 68%]. Stoichiometric amounts of the respective porphyrin component (10 mmol) and of the organic ligand (either 5 mmol or 10 mmol) were dissolved in 3–4 ml of chloroform which turned out to be the preferred solubilizing agent, and mixed. To the resulting solution was added about 1 ml of nitrobenzene (known to be a very effective template for the preparation of crystalline porphyrin solids),[6,16] and this was allowed to crystallize by slow evaporation. This applies also to compound **15**, that yielded a ligand-free material. The resulting solids were fully characterized by crystallographic analyses.

Crystallography

All diffraction measurements were carried out on a Nonius KappaCCD diffractometer using graphite monochromated MoKα radiation (λ = 0.7107 Å). The crystalline samples of the

analyzed compounds were covered with a thin layer of light oil and cooled to 110 K in order to minimize structural disorder and thermal motion effects, and increase the precision of the results. This allowed the location of most of the hydrogen atoms of the porphyrin network in residual electron density maps. The structures were solved using direct methods (SHELXS-86 and SIR-92) and refined by full-matrix least-squares on F^2 (SHELXL-97).[21] Hydrogen atoms were refined using a riding model with fixed thermal parameters [$U_{ij} = 1.2\ U_{ij}$ (eq.) for the atom to which they are bonded].

Compound 8. $C_{44}H_{28}N_4Zn\cdot\frac{1}{2}(C_{14}H_8N_2)\cdot 2(C_6H_5NO_2)$, M = 1026.4, triclinic, space group $P\bar{1}$, a = 11.1700(2), b = 11.6570(3), c = 20.3640(5) Å, α = 82.430(1), β = 76.177(1), γ = 71.857(1)°, V = 2442.0(1) Å^3, Z = 2, D_c = 1.396 g cm^{-3}, μ(MoKα) = 0.56 mm^{-1}, 10675 unique reflections to $2\theta_{max}$ = 55.8°, 676 refined parameters, R_1 = 0.055 for 6622 observations with $I > 2\sigma(I)$, R_1 = 0.113 (wR_2 = 0.135) for all unique data.

Compound 9. $2[C_{44}H_{28}N_4Zn\cdot\frac{1}{2}(C_{12}H_{10}N_4)]\cdot 7(C_6H_5NO_2)$, M = 2432.2, triclinic, space group $P\bar{1}$, a = 10.7210(2), b = 23.5620(3), c = 23.3990(5) Å, α = 70.762(1), β = 87.649(1), γ = 81.944(1)°, V = 5761.7(2) Å^3, Z = 2, D_c = 1.402 g cm^{-3}, μ(MoKα) = 0.50 mm^{-1}, 19484 unique reflections to $2\theta_{max}$ = 50.7°, 1718 refined parameters, R_1 = 0.059 for 12999 observations with $I > 2\sigma(I)$, R_1 = 0.097 (wR_2 = 0.163) for all unique data. There are two crystallographically independent porphyrin and ligand species in the asymmetric unit. Out of the seven nitrobenzene species of the asymmetric unit, five molecules are ordered and two are severely disordered.

Compound 10. $C_{44}H_{28}N_4Zn\cdot\frac{1}{2}(C_{14}H_{14}N_4)\cdot 2(C_6H_5NO_2)$, M = 1043.4, triclinic, space group $P\bar{1}$, a = 10.8810(1), b = 11.7170(1), c = 20.7040(3) Å, α = 96.575(1), β = 91.753(1), γ = 107.380(1)°, V = 2496.7(1) Å^3, Z = 2, D_c = 1.388 g cm^{-3}, μ(MoKα) = 0.55 mm^{-1}, 11606 unique reflections to $2\theta_{max}$ = 56.8°, 685 refined parameters, R_1 = 0.042 for 9136 observations with $I > 2\sigma(I)$, R_1 = 0.063 (wR_2 = 0.108) for all unique data.

Compound 11. $C_{44}H_{28}N_4Zn\cdot\frac{1}{2}(C_{18}H_{14}N_4)\cdot CHCl_3$, M = 940.6, monoclinic, space group $P2_1/n$, a = 9.8790(2), b = 20.2630(5), c = 22.5490(7) Å, β = 100.117(1)°, V = 4443.6(2) Å^3, Z = 4, D_c = 1.406 g cm^{-3}, μ(MoKα) = 0.78 mm^{-1}, 8077 unique reflections to $2\theta_{max}$ = 50.7°, 613 refined parameters, R_1 = 0.072 for 4674 observations with $I > 2\sigma(I)$, R_1 = 0.148 (wR_2 = 0.181) for all unique data. The chloroform solvent exhibits orientational disorder in the crystal lattice.

Compound 12. $C_{44}H_{28}N_4Zn\cdot(C_4H_4N_2O)\cdot 2\frac{1}{2}(C_6H_5NO_2)$, M = 1081.9, triclinic, space group $P\bar{1}$, a = 11.0050(2), b = 11.8750(2), c = 20.6140(5) Å, α = 89.445(1), β = 84.194(1), γ = 71.364(1)°, V = 2538.8(1) Å^3, Z = 2, D_c = 1.415 g cm^{-3}, μ(MoKα) = 0.55 mm^{-1}, 11439 unique reflections to $2\theta_{max}$ = 56.8°, 791 refined parameters, R_1 = 0.061 for 9210 observations with $I > 2\sigma(I)$, R_1 = 0.080 (wR_2 = 0.155) for all unique data. Of the nitrobenzene solvent, one molecule is ordered, another molecule is located on and disordered about the inversion center, and the third species is orientationally disordered.

In structures **8**–**12** the ligand-bridged porphyrin dimers are located on crystallographic centers of inversion.

Compound 13. $(C_{44}H_{28}N_4Mn)^+\cdot(ClO_4)^-\cdot(C_{12}H_{10}N_4)\cdot 3(C_6H_5NO_2)$, M = 1346.7, triclinic, space group $P1$, a = 11.0070(4), b = 11.3980(4), c = 14.2290(5) Å, α = 112.870(2), β = 97.877(1), γ = 96.658(2)°, V = 1601.0(1) Å^3, Z = 1, D_c = 1.397 g cm^{-3}, μ(MoKα) = 0.32 mm^{-1}, 6633 unique reflections to $2\theta_{max}$ = 55.0°, 872 refined parameters, R_1 = 0.045 for 5505 observations with $I > 2\sigma(I)$, R_1 = 0.061 (wR_2 = 0.108) for all unique data. The structure is a racemic twin.

Compound 14. $C_{44}H_{28}N_4Zn\cdot(C_4H_{10}N_4)\cdot 2(C_6H_5NO_2)$, M = 1038.4, monoclinic, space group $P2_1/n$, a = 11.0670(3), b = 9.1590(2), c = 24.9030(7) Å, β = 99.122(1)°, V = 2492.3(2) Å^3, Z = 2, D_c = 1.384 g cm^{-3}, μ(MoKα) = 0.55 mm^{-1}, 5862 unique reflections to $2\theta_{max}$ = 55.7°, 413 refined parameters, R_1 = 0.077 for 3951 observations with $I > 2\sigma(I)$, R_1 = 0.120 (wR_2 = 0.225) for all unique data. The solvent species exhibit a marked disorder. The porphyrin and the ligand components reside on centers of inversion. However, the zinc ion exhibits a twofold disorder about the inversion, deviating above and below the porphyrin plane. The diffraction pattern exhibits a 2/m symmetry with a distinctly centric intensity distribution. However, to ensure that the observed disorder of the central zinc ion is not imposed by the choice of the centrosymmetric space group we have solved and refined the structure in the related space groups $P2_1$ and Pn as well. Yet, these calculations showed similar disorder of the zinc–porphyrin structure.

Compound 15. $2(C_{40}H_{24}N_8Zn)\cdot 5(C_6H_5NO_2)$, M = 1979.6, triclinic, space group $P\bar{1}$, a = 14.818(1), b = 17.076(1), c = 20.135(1) Å, α = 103.486(2), β = 98.214(2), γ = 106.036(5)°, V = 4642.9(4) Å^3, Z = 2, D_c = 1.416 g cm^{-3}, μ(MoKα) = 0.59 mm^{-1}, 17212 unique reflections to $2\theta_{max}$ = 52.9°, 1270 refined parameters, R_1 = 0.106 for 8203 observations with $I > 2\sigma(I)$, R_1 = 0.21 (wR_2 = 0.31) for all unique data. There are two different zinc–porphyrins in the asymmetric unit. The relatively high percentage of low-intensity data is attributed to the high content and considerable disorder of the nitrobenzene solvent in the crystal lattice. This disorder could not be reliably resolved, and the nitrobenzenes were thus geometrically constrained in the refinement. Subtraction of the solvent contribution to the diffraction pattern by the Bypass[22] procedure resulted in a considerably improved convergence of the main supramolecular porphyrin framework at R_1 = 0.074 for 7636 observations above the intensity threshold, and R_1 = 0.145 (wR_2 = 0.191) for 17212 unique data, thus confirming the correctness of the porphyrin structural model.

CCDC reference numbers 165275–165282.

See http://www.rsc.org/suppdata/dt/b1/b104961p/ for crystallographic data in CIF or other electronic format.

Acknowledgements

This research was supported in part by The Israel Science Foundation founded by the Israel Academy of Sciences & Humanities, as well as by Grant No. 1999082 from the United States-Israel Binational Science Foundation (BSF), Jerusalem, Israel.

References

1 V. S.-Y. Lin, S. G. DiMagno and M. J. Therien, *Science*, 1994, **264**, 1105; S. Prathapan, T. E. Johnson and J. S. Lindsey, *J. Am. Chem. Soc.*, 1993, **115**, 7519.

2 J. K. M. Sanders, N. Bampos, Z. Clyde-Watson, S. L. Darling, J. C. Hawley, H.-J. Kim, C. C. Mak and S. J. Webb, in *The Porphyrin Handbook*, ed. K. M. Kadish, K. M. Smith, R. Guilard, Academic Press, London, 2000, vol. 3, pp. 1–48.

3 S. M. LeCours, H.-W. Guan, S. G. DiMagno, C. H. Wang and M. J. Therien, *J. Am. Chem. Soc.*, 1996, **118**, 1497; U. Michelsen and C. J. Hunter, *Angew. Chem., Int. Ed.*, 2000, **39**, 764; S. L. Darling, E. Stulz, N. Feeder, N. Bampos and J. K. M. Sanders, *New. J. Chem.*, 2000, **24**, 261 and references cited therein.

4 C. M. Drain, X. Shi, T. Milic and F. Nifiatis, *Chem. Commun.*, 2001, 287; C. M. Drain, F. Nifiatis, A. Vasenko and J. D. Batteas, *Angew. Chem., Int. Ed.*, 1998, **37**, 2344; P. J. Stang, J. Fan and B. Olenyuk, *Chem. Commun.*, 1997, 1453.

5 E. J. Brandon, R. D. Rogers, B. M. Burkhart and J. S. Miller, *Chem. Eur. J.*, 1998, **4**, 1938; E. J. Brandon, D. K. Rittenberg, A. M. Arif and J. S. Miller, *Inorg. Chem.*, 1998, **37**, 3376; J. S. Miller, J. C. Calabrese, R. S. McLean and A. J. Epstein, *Adv. Mater.*, 1992, **4**, 498.

6 I. Goldberg, *Chem. Eur. J.*, 2000, **6**, 3863; Y. Diskin-Posner, S. Dahal and I. Goldberg, *Angew. Chem., Int. Ed.*, 2000, **39**, 1288; Y. Diskin-Posner and I. Goldberg, *Chem. Commun.*, 1999, 1961.
7 P. N. Taylor and H. L. Anderson, *J. Am. Chem. Soc.*, 1999, **121**, 11538; B. G. Maiya, N. Bampos, A. Asok Kumar, N. Feeder and J. K. M. Sanders, *New. J. Chem.*, 2001, **25**, 797; N. Bampos, V. Marvaud and J. K. M. Sanders, *Chem. Eur. J.*, 1998, **4**, 335.
8 R. Krishna Kumar, Y. Diskin-Posner and I. Goldberg, *J. Inclusion Phenom.*, 2000, **37**, 219; A. D. Shukla, P. C. Dave, E. Suresh, A. Das and P. Dastidar, *J. Chem. Soc., Dalton Trans.*, 2000, 4459.
9 M. P. Byrn, C. J. Curtis, Y. Hsiou, S. I. Khan, P. A. Sawin, S. K. Tendick, A. Terzis and C. E. Strouse, *J. Am. Chem. Soc.*, 1993, **115**, 9480 and references cited therein.
10 H.-J. Kim, N. Bampos and J. K. M. Sanders, *J. Am. Chem. Soc.*, 1999, **121**, 8120; K. Campbell, R. McDonald, N. R. Branda and R. R. Tykwinski, *Org. Lett.*, 2001, **3**, 1045.
11 M. J. Plater, S. Aiken and G. Bourhill, *Tetrahedron. Lett.*, 2001, **42**, 2225; D. Su, X. Wang, M. Simard and J. D. Wuest, *Supramol. Chem.*, 1995, **6**, 171; L. Vaillancourt, M. Simard and J. D. Wuest, *J. Org. Chem.*, 1998, **63**, 9746 (the free-energy of the H-bonding between two molecules of **6** in $CDCl_3$ was determined to be -3.6 kcal mol^{-1}).
12 R. Krishna Kumar, S. Balasubramanian and I. Goldberg, *Chem. Commun.*, 1998, 1435.
13 A survey of the Cambridge Crystallographic Database [F. H. Allen and O. Kennard, *Chem. Des. Automat. News*, 1993, **8**, 31], indicates that only about 20% out of nearly 1500 crystal structures of Zn^{II} complexes known to date contain a six-coordinate zinc ion.
14 P. Dastidar, H. Krupitsky, Z. Stein and I. Goldberg, *J. Inclusion Phenom.*, 1996, **24**, 241.
15 R. Krishna Kumar, S. Balasubramanian and I. Goldberg, *Inorg. Chem.*, 1998, **37**, 541; R. Krishna Kumar and I. Goldberg, *Angew. Chem., Int. Ed.*, 1998, **37**, 3027; H. Krupitsky, Z. Stein and I. Goldberg, *J. Inclusion Phenom.*, 1994, **18**, 177 (identically structured coordination polymers, with other metal ions have been reported more recently: K.-J. Lin, *Angew. Chem., Int. Ed.*, 1999, **38**, 2730).
16 B. F. Abrahams, B. F. Hoskins, D. M. Michail and R. Robson, *Nature (London)*, 1994, **369**, 727.
17 **CAUTION!** Although we have not experienced any problems in dealing with systems containing the perchlorate ion, they can explode spontaneously and should be handled in small quantities at or below room-temperature only. For additional safety precautions see: W. C. Wolsey, *J. Chem. Educ.*, 1973, **50**, A335; W. C. Wolsey, *Chem. Eng. News*, 1983, **61**, 4.
18 S. Hunig, J. Gross, E. F. Lier and H. Quast, *Liebigs Ann. Chem.*, 1973, 339.
19 D. H. Busch and J. C. Bailar, *J. Am. Chem. Soc.*, 1956, **78**, 1137.
20 M. D. Luque de Castro and M. Valcarcel, *Anal. Lett., Part A*, 1978, **11**, 1; S. S. S. Raj, H.-K. Fun, J. Zhang, R.-G. Xiong and X.-Z. You, *Acta Crystallogr., Sect. C*, 2000, **56**, e274.
21 G. M. Sheldrick, SHELXS-86, *Acta Crystallogr., Sect. A*, 1990, **46**, 467; A. Altomare, M. C. Burla, M. Camalli, M. Cascarano, C. Giacovazzo, A. Guagliardi and G. Polidori, SIR-92, *J. Appl. Crystallogr.*, 1994, **27**, 435; G. M. Sheldrick, SHELXL-97, Program for the Refinement of Crystal Structures from Diffraction Data, University of Göttingen, Germany, 1997.
22 P. Van der Sluis and A. L. Spek, *Acta Crystallogr., Sect. A*, 1990, **46**, 194; A. L. Spek, *Acta Crystallogr., Sect. A*, 1990, **46**, C34.